J Geod (2015) 89:775–791
DOI 10.1007/s00190-015-0814-4

ORIGINAL ARTICLE

CODE's new solar radiation pressure model for GNSS orbit determination

D. Arnold[1] · M. Meindl[2] · G. Beutler[1] · R. Dach[1] · S. Schaer[3] · S. Lutz[3] · L. Prange[1] · K. Sośnica[1,4] · L. Mervart[5] · A. Jäggi[1]

Received: 19 December 2014 / Accepted: 8 April 2015 / Published online: 12 May 2015

Abstract The Empirical CODE Orbit Model (ECOM) of the Center for Orbit Determination in Europe (CODE), which was developed in the early 1990s, is widely used in the International GNSS Service (IGS) community. For a rather long time, spurious spectral lines are known to exist in geophysical parameters, in particular in the Earth Rotation Parameters (ERPs) and in the estimated geocenter coordinates, which could recently be attributed to the ECOM. These effects grew creepingly with the increasing influence of the GLONASS system in recent years in the CODE analysis, which is based on a rigorous combination of GPS and GLONASS since May 2003. In a first step we show that the problems associated with the ECOM are to the largest extent caused by the GLONASS, which was reaching full deployment by the end of 2011. GPS-only, GLONASS-only, and combined GPS/GLONASS solutions using the observations in the years 2009–2011 of a global network of 92 combined GPS/GLONASS receivers were analyzed for this purpose. In a second step we review direct solar radiation pressure (SRP) models for GNSS satellites. We demonstrate that only even-order short-period harmonic perturbations acting along the direction Sun-satellite occur for GPS and GLONASS satellites, and only odd-order perturbations acting along the direction perpendicular to both, the vector Sun-satellite and the spacecraft's solar panel axis. Based on this insight we assess in the third step the performance of four candidate orbit models for the future ECOM. The geocenter coordinates, the ERP differences w. r. t. the IERS 08 C04 series of ERPs, the misclosures for the midnight epochs of the daily orbital arcs, and scale parameters of Helmert transformations for station coordinates serve as quality criteria. The old and updated ECOM are validated in addition with satellite laser ranging (SLR) observations and by comparing the orbits to those of the IGS and other analysis centers. Based on all tests, we present a new extended ECOM which substantially reduces the spurious signals in the geocenter coordinate z (by about a factor of 2–6), reduces the orbit misclosures at the day boundaries by about 10 %, slightly improves the consistency of the estimated ERPs with those of the IERS 08 C04 Earth rotation series, and substantially reduces the systematics in the SLR validation of the GNSS orbits.

Keywords GPS · GLONASS · Solar radiation pressure · ECOM

✉ D. Arnold
daniel.arnold@aiub.unibe.ch

[1] Astronomical Institute, University of Bern, Sidlerstrasse 5, 3012 Bern, Switzerland

[2] Institute of Geodesy and Photogrammetry, ETH Zurich, Robert-Gnehm-Weg 15, 8093 Zürich, Switzerland

[3] Federal Office of Topography, Seftigenstrasse 264, 3084 Wabern, Switzerland

[4] Present Address: Institute of Geodesy and Geoinformatics, Wrocław University of Environmental and Life Sciences, Grunwaldzka 53, 50-357 Wrocław, Poland

[5] Institute of Advanced Geodesy, Czech Technical University, K-152, FSvCVVT, Thakurova 7, 16629 Prague 6-Dejvice, Czech Republic

1 Introduction

The Center for Orbit Determination in Europe (CODE)—a joint venture of the Astronomical Institute of the University of Bern, the Federal Office of Topography swisstopo in Wabern, the Federal Agency for Cartography and Geodesy in Frankfurt am Main, and the Institut für Astronomische und Physikalische Geodäsie of the Technische Uni-

versität München—hosts one of the global analysis centers of the International GNSS Service (IGS, Dow et al. 2009).

The Empirical CODE Orbit Model (ECOM, Beutler et al. 1994) was developed in the early 1990s, motivated by the lack of reliable satellite information. The attempt was made to solve for the minimum number of solar radiation pressure (SRP) parameters using readily available a priori models, first the ROCK-T models until November 2005 and then a model derived from the parameters of the ECOM (Springer et al. 1999a; Dach et al. 2009). Since July 2013 the ECOM is used at CODE without any a priori SRP model, after having implemented albedo modeling. With the deployment of more and more GLONASS satellites, problems were slowly developing and it became clear that the ECOM has shortcomings and needs a thorough review. This was confirmed in the article by Meindl et al. (2013) and is in line with Rodríguez-Solano et al. (2014b).

It was thus clear that something had to be done to improve the situation. The simplest, and probably most effective corrective action would have been to abandon the analysis of GLONASS data (see Sect. 3.2). In view of the large user community relying on the CODE combined products this was, however, not considered a valuable option. Furthermore, the classic ECOM has problems to sufficiently parametrize the orbits of GLONASS satellites because the bodies of the latter are, in contrast to GPS satellites, of a markedly elongated shape. As this is the case for other satellites (like the European GNSS Galileo) as well, the decision to simply restrict the ECOM to GPS satellites would not have been sustainable.

It is, therefore, the main purpose of this article to review the ECOM, which was successfully applied by CODE and other IGS analysis centers in the past 20 years and to make it fit for the next 20 years. It shall be updated to better account also for the SRP characteristics of the GLONASS and other GNSS satellites.

Section 2 reviews essential developments of SRP modeling in the IGS environment. Section 3 first reviews the ECOM as it was used until now and then shows that the classical ECOM is even today a good model when analyzing GPS-only data and that its problems are caused to the greatest extent by GLONASS. Interestingly, the ECOM problems may be substantially reduced, if a particular parameter type of the ECOM is not estimated for the GLONASS satellites. Section 4 first assembles the elements underlying the proposed modified ECOM and then presents its most general form. Section 5 introduces the candidates considered for the new ECOM and analyzes their performance. Section 6 validates the candidate ECOM models using the observations conducted by the International Laser Ranging Service (ILRS) as described in Pearlman et al. (2002). Section 7 summarizes the findings and presents the orbit model selected for the future CODE contributions.

2 Orbit modeling activities in the IGS environment

Fliegel et al. (1992, 1996) pioneered the development of a priori models to account for SRP for the GPS satellites. Models for Block I, Block II, and Block IIA were presented in Fliegel et al. (1992), whereas the model for the Block IIR satellites was provided in 1996—at a time when no Block IIR satellite was yet in orbit. The so-called standard ROCK-S models without and the ROCK-T models with thermal re-radiation and other modeling improvements, were provided for Blocks II and IIA. The perturbing accelerations were given in the form of a Fourier expansion in the body-fixed coordinates X and Z, using the angle between the Sun and the spacecraft's Z axis, as seen from the center of the satellite, as angular argument. The geodetic community was advised to use ROCK-T, to estimate a scaling factor of the model accelerations, and to solve for the so-called Y bias (Fliegel et al. 1992). This advice was generally accepted in the early 1990s. The Fliegel publications set the standard for many future developments.

Ziebart et al. (2002) make the distinction between analytical SRP models, analytical models with empirical scaling or augmentation, and empirical models. They are strong advocates of analytical modeling, which makes sense as this reduces potential correlations between orbit and other parameters. However, this requires that for all satellites processed there is sufficient and reliable information about the satellite's surface properties, their thermal behavior, and their attitude available.

Bar-Sever et al. (2004) follow a different approach for SRP modeling. Their model is in essence based on the Fliegel formulation, introduces additional terms, and, most importantly, empirically determines the parameters using a least squares fit to long chains of daily orbits computed by JPL.

The development of the Empirical CODE Orbit Model by Beutler et al. (1994) was motivated by the necessity to solve for more than just a scaling factor for the ROCK-T models and by the concern that the force signatures introduced by a priori models could not be removed by estimating only a scale factor. The ECOM decomposes the perturbing acceleration into three orthogonal directions well adapted to SRP modeling and adopts a truncated Fourier series expansion for each component using the satellite's argument of latitude as the angular argument.

Springer (1999b) used the ECOM and proposed what is called today the reduced ECOM, which just solves for the three zero-order terms of the expansion and the first-order term in one of the components. The author showed that the orbits improved as a consequence of this particular parametrization. Springer et al. (1999a) published the key findings, where they also presented the coefficients of an alternative a priori model, based uniquely on the ECOM. The reduced ECOM was successfully used by CODE and others until

2014. At CODE, it was first used on top of the ROCK-T models, then on top of an ECOM-derived a priori model, and eventually, since mid 2013, without any a priori model at all.

In recent years it became evident, however, that the ECOM suffers from shortcomings. Meindl (2011) used a worldwide network of 92 combined GPS/GLONASS receivers to study the properties of GPS-only, GLONASS-only, and combined GPS/GLONASS solutions. It became clear that since about 2009 high-accuracy global products, namely GNSS orbits, Earth rotation parameters (ERPs), station coordinates, and geocenter estimates could be generated using only GLONASS observations. It was, however, also clear that some of the GLONASS-only products contained pronounced deviations, which did not show up in the GPS-only products. The effect was particularly prominent in the z-component of the geocenter. Meindl et al. (2013) clearly identified it as a GLONASS-specific artifact and explained the mechanism how it was introduced into the results. The results are based on one and the same orbit model—the reduced ECOM.

Every satellite method of space geodesy has to determine orbit parameters of the observed satellites when solving for global parameters of geophysical interest. Modeling deficits must, therefore, be expected in the geophysical parameters if the force field acting on the satellite is not perfectly known.

Ray et al. (2008) described spurious spectral lines in the spectra of the IGS station coordinates already in 2008—using data when GLONASS did not yet play a significant role in the IGS network. The periods of the spectral lines could be attributed to the so-called draconitic GPS year, which, due to the regression of the satellite nodes on the equator, is about 14 days shorter than the sidereal year. The effects are small: the amplitudes of the spectral lines, which can be reconstructed from the power spectra in Ray et al. (2008, 2013), are only about a factor of 1–3 above the noise level. Griffith and Ray (2012) state that draconitic errors are contained in virtually all IGS products.

Rodríguez-Solano et al. (2014b) documented a significant reduction of the spurious effects in the z-coordinate of geocenter motion, in the ERPs, in the orbit misclosures at the day boundaries, and in the stacked spectra of the station coordinates, by replacing the reduced 5-parameter ECOM for GPS and GLONASS by an adjustable box-wing model, which was developed by Rodríguez-Solano (2014a).

Montenbruck et al. (2014) analyzed the performance of the ECOM when applied to Galileo In-Orbit Validation satellites. The authors related systematic orbit and clock errors to shortcomings of the ECOM when used for the Galileo satellites, the bodies of which are, as opposed to GPS satellites, of a significantly elongated shape (as are the GLONASS satellites). As a consequence, the authors propose an a priori box model which augments the ECOM with parameters adjusted using Galileo observations over an extended time span.

Nonetheless, a purely empirical SRP modeling has several advantages over analytical or semi-analytical approaches. Apart from its simplicity, an empirical SRP model can be easily applied to every satellite without precise knowledge of its shape, mass, attitude, and optical properties of its surfaces. We aim at further retaining this universality and therefore review the ECOM in the light of the mentioned shortcomings. It is our goal to develop an improved ECOM which is better adapted to SRP modeling of all GNSS satellites, including GLONASS

3 The ECOM and its applications to GNSS analysis

We first review the characteristics of the ECOM used until now in Sect. 3.1. We then study its performance in GPS-only, GLONASS-only, and combined GPS/GLONASS analyses in Sect. 3.2.

3.1 The Empirical CODE Orbit Model (ECOM)

All ECOMs decompose the perturbing accelerations into three orthogonal directions

$$\mathbf{e}_D \doteq \frac{\mathbf{r}_\mathrm{s} - \mathbf{r}}{|\mathbf{r}_\mathrm{s} - \mathbf{r}|}, \quad \mathbf{e}_Y \doteq -\frac{\mathbf{e}_r \times \mathbf{e}_D}{|\mathbf{e}_r \times \mathbf{e}_D|}, \quad \mathbf{e}_B \doteq \mathbf{e}_D \times \mathbf{e}_Y, \tag{1}$$

where $\mathbf{r}_\mathrm{s}$ and $\mathbf{r}$ are the geocentric vectors of the Sun and the satellite, respectively, and $\mathbf{e}_r$ is the unit vector associated with $\mathbf{r}$. The vector $\mathbf{e}_D$ is the unit vector in the direction satellite-Sun, $\mathbf{e}_Y$ points along the satellite's solar panels axes, and $\mathbf{e}_B$ completes the orthogonal system. The total acceleration of a satellite due to solar radiation pressure can then be written as

$$\mathbf{a} = \mathbf{a}_0 + D(u)\mathbf{e}_D + Y(u)\mathbf{e}_Y + B(u)\mathbf{e}_B, \tag{2}$$

where $\mathbf{a}_0$ is a selectable a priori model, and where u is the satellite's argument of latitude (Fig. 1).

In the original ECOM the functions $D(u)$, $Y(u)$ and $B(u)$ are represented as Fourier series truncated after the once-per-revolution (1pr) terms,

$$\begin{aligned} D(u) &= D_0 + D_\mathrm{c}\cos u + D_\mathrm{s}\sin u \\ Y(u) &= Y_0 + Y_\mathrm{c}\cos u + Y_\mathrm{s}\sin u \\ B(u) &= B_0 + B_\mathrm{c}\cos u + B_\mathrm{s}\sin u, \end{aligned} \tag{3}$$

using the satellite's argument of latitude u as angular argument.

The decomposition (1) and the SRP model (2), (3) were proposed by Beutler et al. (1994). Since 1996 the model has been used by the CODE Analysis Center of the IGS.

The ECOM actually used by CODE is the so-called reduced ECOM (Springer et al. 1999a):

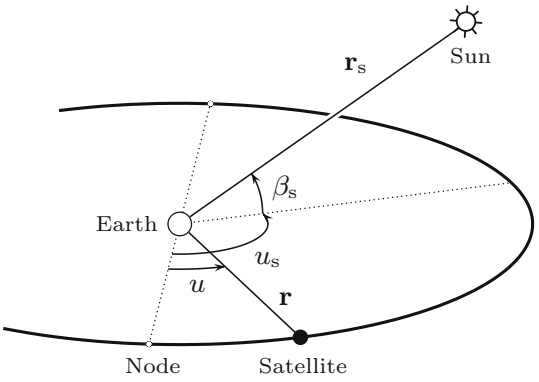

Fig. 1 Satellite-geocenter-Sun geometry. u_s and β_s denote the argument of latitude and the elevation angle of the Sun w.r.t. the orbital plane

$$
\begin{aligned}
D(u) &= D_0 \\
Y(u) &= Y_0 \\
B(u) &= B_0 + B_c \cos u + B_s \sin u. \qquad (4)
\end{aligned}
$$

Furthermore, since July 2013, no a priori model is used for the CODE IGS contributions, i.e., $\mathbf{a}_0 = \mathbf{0}$.

The term 'empirical model' may have different meanings. It is sometimes used as a label for a model the parameters of which are fit to data and which is used as a priori model. Here, we use the term to characterize the parametrization (2).

3.2 GPS-only, GLONASS-only, and combined GPS/GLONASS solutions

Meindl (2011) analyzed GPS-only, GLONASS-only, and combined GPS/GLONASS data of the years 2008–2010 from a global network exclusively consisting of 92 combined GPS/GLONASS receivers. Meindl et al. (2013) added the year 2011 to this data set to study the series of geocenter coordinates of GLONASS-only and GPS-only solutions. In our analysis we skip the year 2008, because at that time the GLONASS-only solution still suffered from the incomplete GLONASS constellation. Here, we broaden the investigation by studying the quality of the ERPs, as well.

The analysis is closely related to that of the CODE IGS one-day solutions: orbits, station coordinates, ERPs, and geocenter coordinates are estimated together with other parameters like troposphere zenith delays and remaining unresolved ambiguities. The reduced ECOM (4) of the CODE routine analysis was used by Meindl et al. (2013) and for the first half of this section. No a priori orbit model was applied.

Figures of the geocenter coordinates for the three solution series may be found in Meindl et al. (2013). Figure 2 shows the spectral decomposition of the geocenter motion in the z-coordinate, which is—in contrast to the other two components—known to be most sensitive to orbit modeling issues.

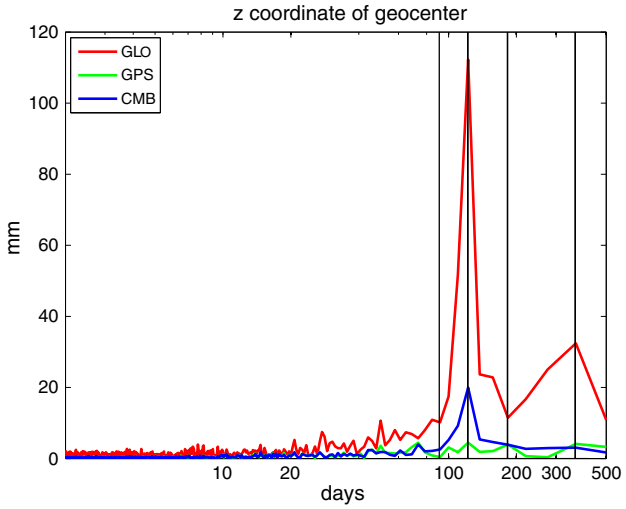

Fig. 2 Amplitude spectra of the geocenter z-coordinate 2009–2011 as estimated from the GLONASS-only (GLO), GPS-only (GPS), and combined GPS/GLONASS (CMB) solutions

The vertical lines in Fig. 2 and in subsequent spectra mark the annual, semi-annual etc. periods. The differences between the tropical year and the draconitic year of GPS and GLONASS cannot be resolved for our comparatively short time period of three years.

The dominating phenomenon in Fig. 2 is the spectral line with an amplitude of 112 mm at three cycles per year (3 cpy) in the GLONASS-only solution. This massive signal was the motivation for Meindl et al. (2013) to study geocenter motion.

The GPS-only solution has an amplitude of about 4 mm at this frequency, whereas the combined GPS/GLONASS solution still has an amplitude of 20 mm, which, therefore, must be GLONASS-induced.

Table 1 lists the amplitudes of the spectral lines of the geocenter coordinates at the frequencies of 1, 2, and 3 cpy for all solutions considered in this section: the column entitled B_{1pr} indicates whether the 1pr terms in the B-component of Eq. (4) were actually estimated or not. 'yes' means that the terms are estimated for all satellites; 'no' that they are estimated for no satellite; and 'GPS' that they are estimated for GPS satellites only. Experiments with $B_{1pr} \neq$ yes will be discussed in the second half of this section.

The results for the x- and y-components of the GPS, GLONASS, and the combined solutions are rather consistent. The consistency is, however, far from an acceptable level for the z-coordinate. It is particularly worrisome that the amplitude at 3 cpy in the combination is still biased to a value five times larger than in the GPS-only solution.

The polar motion coordinates x and y, their drifts, and the length of day (LOD) are accessible parameters to satellite geodetic methods. When only analyzing orbital arcs of one day, as it is done in the IGS since 2012, it does not make sense to study the polar motion drifts, because their determination is very weak. This aspect was discussed by Hefty et al. (2000),

Table 1 Amplitudes (in mm) of the geocenter coordinates

Par	Sys	B_{1pr}	3 cpy	2 cpy	1 cpy
x	GLO	yes	2	1	9
x	GPS	yes	1	0	7
x	CMB	yes	1	1	8
y	GLO	yes	2	2	5
y	GPS	yes	1	2	10
y	CMB	yes	1	2	9
z	GLO	yes	112	11	32
z	GPS	yes	4	4	4
z	CMB	yes	20	4	3
x	GLO	no	2	9	7
x	GPS	no	1	5	9
x	CMB	no	1	2	8
y	GLO	no	2	6	3
y	GPS	no	1	1	8
y	CMB	no	1	2	7
z	GLO	no	11	6	34
z	GPS	no	4	4	18
z	CMB	no	3	5	19
x	CMB	GPS	0	2	7
y	CMB	GPS	1	1	8
z	CMB	GPS	4	5	11

who pointed out that polar motion estimates with a higher than daily resolution require special measures. Mean errors of the polar motion drifts of several 100 μas/day confirm these findings. Therefore, we decided to focus subsequently only on the quality of the pole coordinates x and y, and of LOD.

Figures 3 and 4 show the amplitude spectra of the x- and y-pole coordinate differences and of LOD differences of the three solutions w. r. t. the IERS 08 C04 series (Bizouard et al. 2009). Assuming that the IERS values are true, all differences should be zero and the spectrum should not show amplitudes above the noise level. The reference series is not really independent of the solutions discussed here, because GNSS solutions based on similar sets of observations were used for their generation—together with the results of the other space geodetic techniques. It is, however, the best reference available for our purpose.

Table 2 contains the amplitudes at 1, 2, 3, and 4 cpy and the sums of these amplitudes of the polar motion coordinate differences w. r. t. IERS 08 C04. The sum of the four amplitudes represents the maximum possible deviation of the respective ERP differences, provided the differences would be uniquely due to the four spectral lines.

The GLONASS-only solutions are heavily deteriorated in the polar motion coordinates x and y. By far the largest

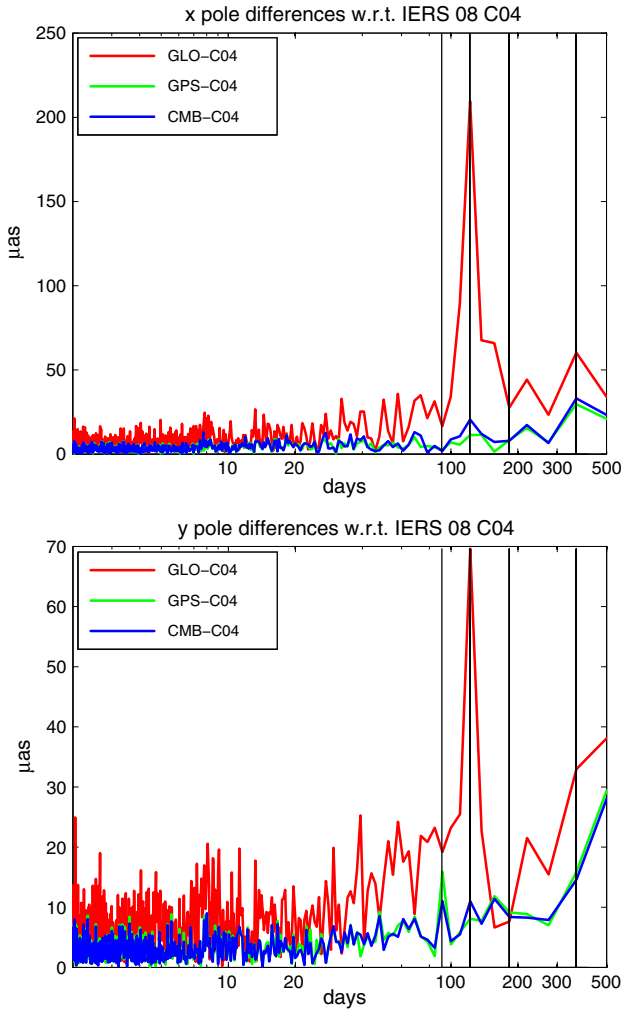

Fig. 3 Amplitude spectra of differences of polar motion coordinates x (*top*) and y (*bottom*) from the GLONASS-only, GPS-only, and combined GPS/GLONASS solutions w. r. t. IERS 08 C04

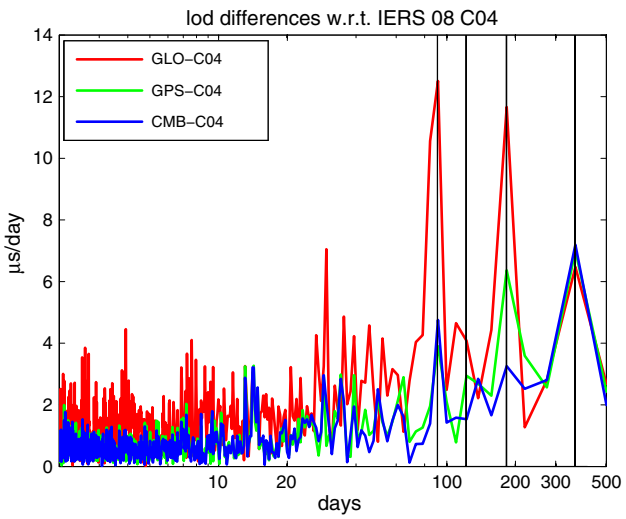

Fig. 4 Amplitude spectra of differences of LOD from the GLONASS-only, GPS-only, and combined GPS/GLONASS solutions w. r. t. IERS 08 C04

Table 2 Amplitudes of polar motion differences (in μas) w. r. t. IERS 08 C04

Par	Sys	B_{1pr}	4 cpy	3 cpy	2 cpy	1 cpy	Sum
x	GLO	yes	16	210	28	60	314
x	GPS	yes	3	11	8	30	52
x	CMB	yes	2	20	8	33	63
y	GLO	yes	19	70	8	33	130
y	GPS	yes	16	8	9	16	49
y	CMB	yes	11	11	8	15	45
x	GLO	no	18	108	7	23	156
x	GPS	no	8	5	11	24	48
x	CMB	no	6	28	8	23	65
y	GLO	no	6	21	18	57	102
y	GPS	no	22	4	5	4	35
y	CMB	no	12	5	9	7	33
x	CMB	GPS	3	26	2	19	50
y	CMB	GPS	11	6	7	6	30

Table 3 Amplitudes of LOD differences (in μs/day) w. r. t. IERS 08 C04

Sys	B_{1pr}	4 cpy	3 cpy	2 cpy	1 cpy	Sum
GLO	yes	12.5	4.1	11.7	6.5	34.8
GPS	yes	3.9	2.9	6.4	7.0	20.2
CMB	yes	4.8	1.5	3.3	7.2	16.8
GLO	no	9.2	4.0	9.0	5.6	27.8
GPS	no	2.4	1.9	2.5	8.4	15.2
CMB	no	3.1	2.9	2.6	7.0	15.6
CMB	GPS	3.8	2.5	2.1	6.6	15.0

amplitude is encountered in the x-coordinate at the frequency of 3 cpy. The sum of the amplitudes of these differences are about 314 and 130 μas in the x- and y-coordinates, respectively. The corresponding values for the GPS-only solution are 52 and 49 μas, respectively. The combination of the x-component is clearly contaminated, whereas the effect is smaller in the y-component.

The amplitudes of the LOD differences at 4 to 1 cpy and their sums are provided in Table 3. The sum of the amplitudes of the GLONASS-only solution is with 34.8 μs/day roughly 70 % larger than the corresponding GPS-only value, indicating that a GLONASS-induced artifact exists in LOD, as well. Note, however, that the combined solution does not only clearly reduce the GLONASS-only semiannual and quarterly amplitudes, but also the GPS-only semiannual amplitude.

The results discussed so far are valid for the orbit model used by Meindl et al. (2013), the 5-parameter ECOM (4). Subsequently, we further simplify this model by omitting the 1pr terms in B—disregarding the evidence of the usefulness of these terms found by Springer et al. (1999a). This simplified ECOM is motivated by Rodríguez-Solano et al. (2014b), who pointed out that these terms may alter the orbital plane, in addition to the constant term D_0 studied by Meindl et al. (2013).

As it is clear by now that the biases in the combination are mainly caused by GLONASS, we also include a combined solution using the original reduced ECOM (4) for the GPS and the ECOM with only three empirical accelerations, namely the three constant accelerations D_0, Y_0, and B_0, for the GLONASS.

The results of the alternative parametrization are contained in Tables 1, 2, and 3 for the geocenter coordinates, the polar motion components x, y, and LOD, respectively. B_{1pr} = no stands for the solutions adopting the 3-parameter ECOM for all satellites, B_{1pr} = GPS for solutions adopting the 5-parameter ECOM for GPS, and the three-parameter ECOM for GLONASS.

Table 1 reveals that the 3-parameter ECOM has a remarkably positive impact on the GLONASS-only z-coordinate of the geocenter: the amplitude at 3 cpy drops from 112 to 11 mm. Ironically, the terms which had a clearly positive impact on GPS-only solutions according to Springer et al. (1999a) prove to be harmful for GLONASS-only solutions. The effect is also clearly visible in the combined solutions: the amplitude at 3 cpy drops from 20 to 3 mm from B_{1pr} = yes to B_{1pr} = no and stays at 4 mm for B_{1pr} = GPS. Note, however, that the omission of the periodic terms in B induces an increase of the amplitude at 1 cpy. This is most prominent in the GPS-only and combined solutions when not estimating the periodic B terms at all: the amplitudes grow from 4 and 3 mm to 18 and 19 mm, respectively. For the combined solution the increase to 11 mm is a bit smaller when estimating periodic B terms only for GPS.

Table 2 also provides the amplitudes of the polar motion differences of our solutions w. r. t. IERS 08 C04 for B_{1pr} = no and B_{1pr} = GPS. The GLONASS-only solutions without the 1pr terms in B are clearly superior to the conventional solutions: for the x- and y-coordinates the amplitude sums drop from 314 μas and 130 μas to 156 μas and 102 μas, respectively. The improvements for the combined solutions are still visible, but less pronounced.

For GLONASS-only solutions the sum of the amplitudes of the LOD differences w. r. t. IERS 08 C04 drops from 34.8 μs/day for the 5-parameter ECOM to 27.8 μs/day for the 3-parameter ECOM. Again, the advantage is with the solutions without periodic ECOM terms. Interestingly, we also see a slight improvement for the GPS-only LOD values when skipping the 1pr terms in B. This fact was also noted by Springer et al. (1999a).

We have thus seen that for the GLONASS-only solutions the traditional ECOM is clearly inferior in all aspects considered to the solution not solving for the 1pr terms in B.

For GPS the picture is not so clear. For the geocenter estimates the classic model is slightly superior, for the polar motion parameters both models are on the same level, and for LOD the three-parameter ECOM is slightly better.

Our experiments have shown that (a) GLONASS-only solutions suffer from massive artifacts in the geocenter z-coordinate and in all ERP parameters when using the 5-parameter ECOM model of Eq. (4); that (b) GPS-only solutions show no, or at least much smaller spurious signals in the estimated geocenter coordinates and in the ERPs; and that (c) combined GPS/GLONASS solutions based on model (4) contain reduced, but still noticeable GLONASS-induced artifacts.

We are thus facing a GLONASS-specific problem with the reduced ECOM (4). Our results indicate on the one hand an insufficient parametrization for GLONASS orbits and on the other hand an inability to determine the 1pr terms in B without biasing parameters of geophysical interest. Combined solutions solving only for the three constant accelerations for GLONASS, but for all five parameters for GPS, are a promising alternative. In any case, a careful review of the ECOM is necessary; an update of the orbit modeling will eventually allow for a reduction of the described deficits.

4 Expectations from theory

Section 4.1 assembles the essential facts underlying the new extended ECOM and studies the spectral behavior of the ROCK-T and the box-wing models. We assume that the attitude control (yaw-steering mode) of the satellite is perfect. It is well known, on the other hand, that during eclipse seasons this is not the case, neither for GLONASS nor for GPS. We do not, however, address this issue in the present article. In Sect. 4.2 the mathematic foundations of the proposed extended ECOM are laid out.

4.1 Basics of SRP modeling

SRP is caused by momentum transfer of absorbed, emitted, or reflected photons to the satellite. In an analytical SRP modeling approach the satellite's surface is subdivided into individual surfaces—each with its optical properties and orientation—and the theoretical acceleration due to each surface is calculated. The absorbed radiation accelerates the satellite along $-\mathbf{e}_D$. Specularly reflected radiation on a surface element accelerates the satellite along the normal vector of the surface element (pointing into the satellite). Diffusely reflected radiation induces an acceleration in the direction of a vector in the plane spanned by the surface normal vector and $\mathbf{e}_D$. Thermal re-radiation and Earth-albedo radiation have to be taken into account, as well. The total SRP is then obtained by summing up the contributions from all surface elements.

For box-wing-type SRP models (Rodríguez-Solano 2014a) the satellite is described by a small number of surfaces, while Ziebart (2004) established a more complex handling of SRP by finite element representation of the satellite and by ray-tracing techniques.

In contrast to the analytical or semi-analytical models, an empirical SRP model remains independent of the precise shape of the satellite and the optical properties of its surfaces and aims at estimating SRP-induced accelerations in suitable directions. How should an empirical SRP model look like from the perspective of theory? Figure 5 illustrates the relevant geometry. In the figure we are looking edge-on at the satellite's orbital plane from the nodal line of the orbit in the terminator system. The fundamental plane of this system is the terminator, the first axis points out of the plane of projection along the nodal line, and the third axis points always towards the Sun and is parallel to the $\mathbf{e}_D$-axis of the ECOM.

Assuming a perfect attitude, the solar panels are always perpendicular to $\mathbf{e}_D$ and the resulting acceleration attributed to them is constant and pointing in the direction $-\mathbf{e}_D$. This is why—for direct SRP—we focus uniquely on the satellite body from now on.

Figure 5 shows a particularly simple satellite body, a cuboid, operated in a yaw-steering attitude mode (Bar-Sever 1996). This attitude is assumed by many GNSS satellites during non-eclipse phases and can be summarized as follows: the satellite's $+Z$-surface, containing the antenna array,

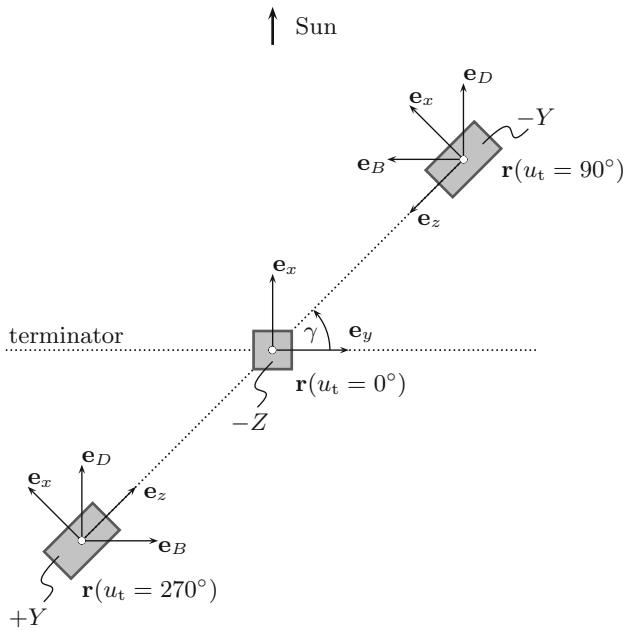

Fig. 5 Cuboid satellite body in terminator system at arguments of latitude $u_t = (0, 90, 270)°$, measured in the terminator system. Z-surface contains the antenna array; X-surface is normal to the satellite-fixed $\mathbf{e}_x$-axis; γ is the elevation of the satellite's orbital plane above the terminator plane. $\gamma = 90° - \beta_s$. The solar panels, which are attached to the surfaces $\pm Y$, are not shown in the figure

always points towards the geocenter and the solar panel axis is always perpendicular to $\mathbf{e}_D$, such that the satellite-fixed vector $\mathbf{e}_x$ points into the half-plane containing the Sun. Hence, for the cuboid of Fig. 5 the Sun never illuminates the surfaces to which the solar panels are attached ($\pm Y$). Direct SRP is thus constrained to the $(\mathbf{e}_B, \mathbf{e}_D)$-plane, where the vectors are defined by Eq. (1). An acceleration along the third ECOM axis $\mathbf{e}_Y$ only occurs, if the satellite is not aligned properly, in particular if the body-fixed Y-axis is not perpendicular to $\mathbf{e}_D$.

Assuming nominal yaw-steering for a cuboid-shaped satellite body with fully symmetric areas and optical properties for the $\pm X$ and $\pm Z$ surfaces and excluding self-shadowing effects, the following basic facts related to direct SRP acting on the satellite body can be seen in Fig. 5:

- For $\beta_s = \pm 90°$ the Sun always illuminates the same cross section of the satellite body, the X-surface of the satellite. Therefore, all periodic variations due to direct SRP must vanish.
- The acceleration in Y-direction completely vanishes; hence the zero-order term Y_0 should also be zero.
- The SRP accelerations are the same for the arguments of latitude $u_t = (0, 180)°$ measured in the terminator system, independent of the β_s-angle.
- For $\beta_s = 0°$, i. e., for $\gamma = 90°$, the overall short-periodic variations over a revolution period assume maximum amplitude.
- We can conclude that (a) the D-component only has even-order periodic terms in u_t and that (b) the B-component only has odd-order periodic terms in u_t.

The statement concerning the orders of the short-periodic perturbations emerges from the fact that—under the assumptions made—the SRP geometry is the same for every pair of angles $(u_t, u_t + 180°)$: as the D-component refers to a fixed axis in an inertial reference frame, only even-order terms can occur; as $\mathbf{e}_B$ rotates by 180° in this system over half of the satellite's revolution period, the B-component can only contain odd-order short-periodic perturbations, and the zero-order term B_0 must be zero.

These predictions from theory can be checked by analyzing the accelerations given by analytical SRP models. For GPS satellites the ROCK-T models (Fliegel et al. 1992, 1996) and the box-wing models (Rodríguez-Solano 2014a) are available to calculate the resulting SRP; for GLONASS only the box-wing models can be used.

Figure 6 shows the accelerations in D and B over one revolution period of a GLONASS satellite for elevation angles

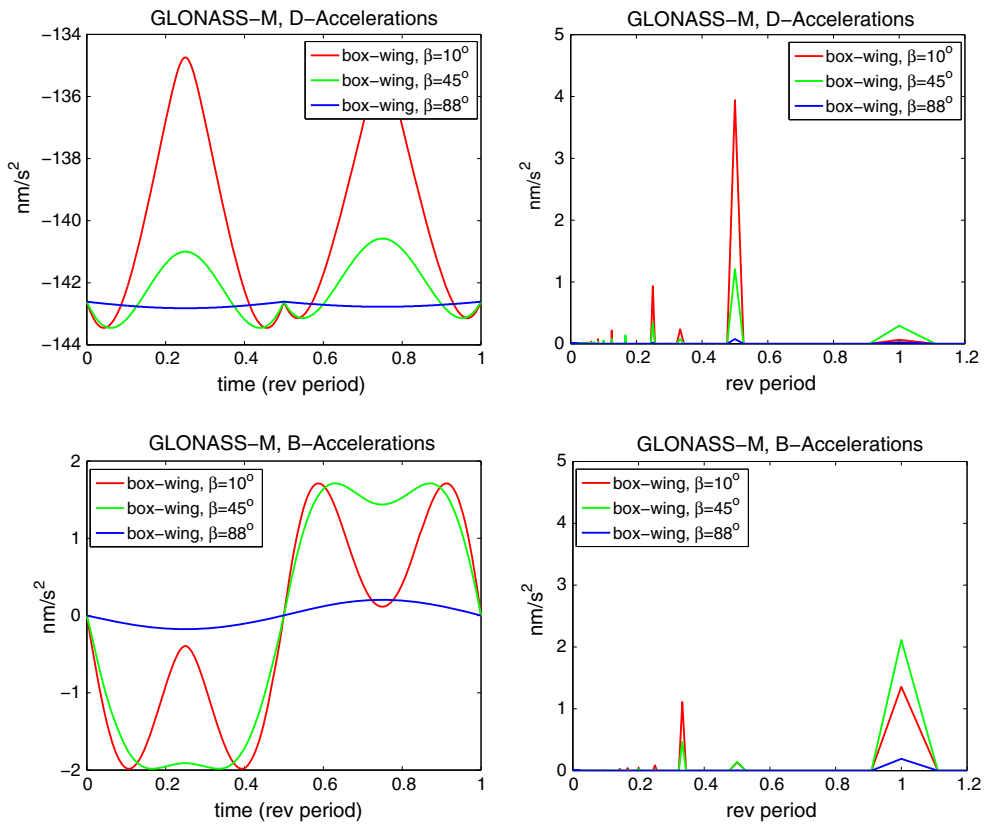

Fig. 6 Box-wing accelerations (Rodríguez-Solano 2014a) for GLONASS-M in D (*left, top*) and B (*left, bottom*), and corresponding amplitude spectra (*right*)

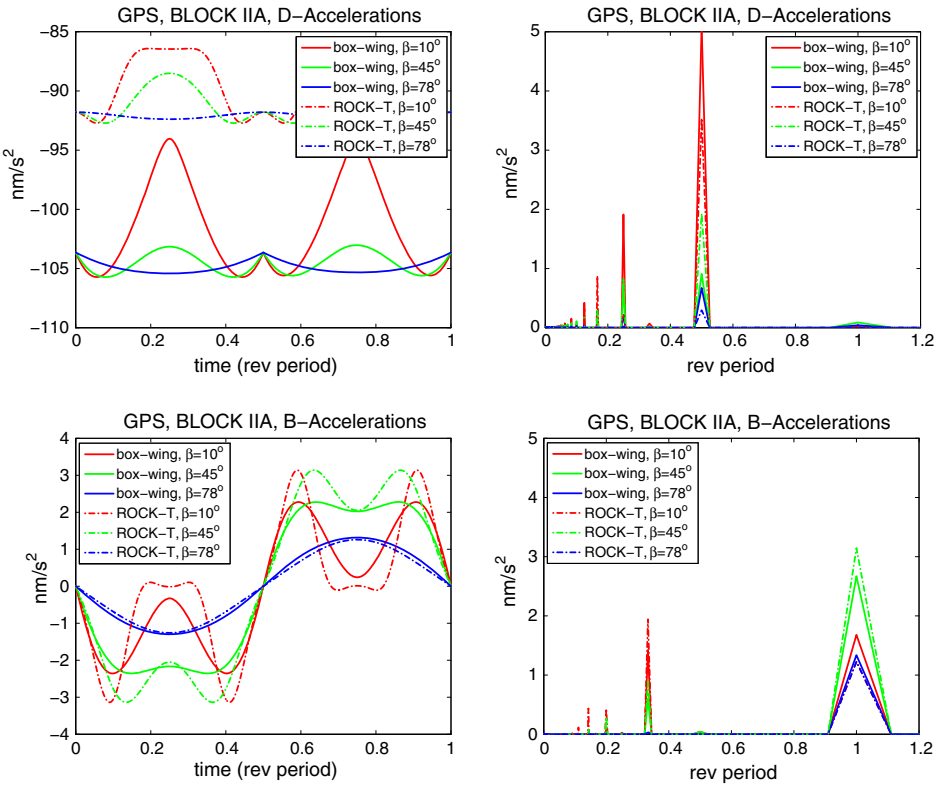

Fig. 7 Box-wing and ROCK-T accelerations for GPS Block IIA in D (*left, top*) and B (*left, bottom*), and corresponding amplitude spectra (*right*)

of $\beta_s = (10, 45, 88)°$ of the Sun above the orbital plane. The highest elevation corresponds to the maximum value possible for GLONASS (Meindl et al. 2013). The accelerations in Y are not shown because they only contain a constant Y-bias.

The above theoretical predictions are almost perfectly met by the box-wing model: sizeable spectral lines only exist for even orders and odd orders in D and B, respectively. Small differences are caused by asymmetries of the satellite body.

The box-wing model predicts a strong twice-per-rev (2pr) signal in D with amplitudes of about 4 nm/s^2 (GLONASS) and 5 nm/s^2 (GPS) for $\beta_s = 10°$ and a significant 1pr signal in B, as well. The 2pr signal in the D acceleration decreases when the angle β_s increases and disappears for $\beta_s \to \pm 90°$. The maximum strength of the 1pr spectral line in B is obtained for $|\beta_s| \approx 45°$. Figure 6 (right) furthermore reveals that apart from the main spectral lines in D and B there are sizeable four-per-rev (4pr) terms in D and three-per-rev (3pr) signals in B.

It is thus a serious defect of the reduced ECOM of Eq. (4) when applied to GLONASS that the 2pr terms in D are neither captured by an a priori model nor estimated. Moreover, an omission of the 1pr term in B cannot be justified from the perspective of theory.

Figure 7 shows the accelerations predicted by the box-wing and ROCK-T models for the GPS Block IIA satellites. We use $\max(\beta_s) \approx 78°$ (Meindl et al. 2013).

The box-wing model gives the Block IIA satellites similar 2pr values in D as for GLONASS-M, whereas the corresponding ROCK-T amplitude is substantially smaller. Both, the box-wing and the ROCK-T models, predict 1pr terms in B with amplitudes of about 3.0 nm/s^2 for $\beta_s \approx 45°$.

Comparisons between ROCK-T and box-wing-models can be generated for GPS Block IIR and Block IIF satellites. The general structure is the same as for the GLONASS-M and GPS Block IIA satellites; only the magnitudes of the spectral lines vary.

Having seen that the theoretical predictions concerning the orders of the perturbations in D and in B are quite well met by the ROCK-T and the box-wing models, we may expand the predicted accelerations in an extended Fourier series with only even-order terms for D and only odd-order terms for B, see Eq. (5). Figure 8 shows the computed coefficients as a function of β_s for GLONASS-M when truncating the series after 8pr and 7pr-terms for D and B, respectively. Note that the coefficients of the cosine terms of the Fourier expansion are shown, while the sine terms are close to zero; see the remark at the end of Sect. 4.2.

The figures have the same scale for D and B. We can thus conclude that the 2pr term in D is larger than the 1pr term in B in absolute value.

Figure 8 (left) suggests that the estimation of the 2pr terms in D is mandatory for GLONASS and that the 4pr terms may be important for small β_s, e. g., $|\beta_s| \leq 30°$. The 6pr and 8pr

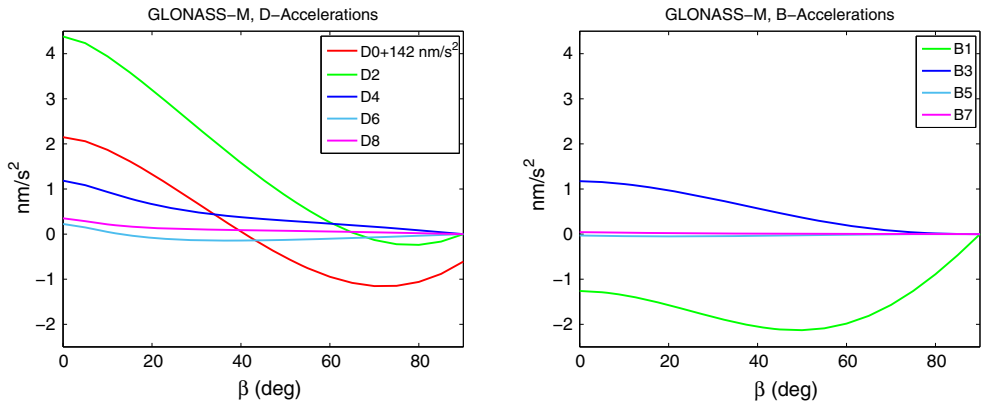

Fig. 8 Coefficients of D-expansion (*left*) and B-expansion (*right*) of box-wing accelerations

terms may safely be omitted. Figure 8 (right) shows that the 1pr term in B is dominant, but that the 3pr term may be as well significant for $|\beta_s| \leq 30°$.

From the perspective of theory we thus conclude that a realistic SRP model must contain periodic terms of even order in D and of odd order in B. For a straightforward interpretation of the estimated ECOM parameters the angular argument $\Delta u = u - u_s = u_t - 90°$ should be used instead of the argument of latitude u referring to the inertial equatorial system.

Finally, we point out that the above considerations were made for direct SRP, i. e., when neglecting thermal re-radiation and Earth-albedo radiation. These (smaller) effects, as well as an incorrect satellite attitude, an asymmetric satellite body, or self-shadowing effects may cause a deviation from the theoretically predicted SRP properties.

4.2 The extended ECOM

We write the components of the extended ECOM as truncated Fourier series with the angular argument $\Delta u \doteq u - u_s$, where u_s is the Sun's argument of latitude in the satellite's orbital plane (Fig. 1):

$$\begin{aligned} D(u) &= D_0 + \sum_{i=1}^{n_D} \left\{ D_{2i,c} \cos 2i\Delta u + D_{2i,s} \sin 2i\Delta u \right\} \\ Y(u) &= Y_0 \\ B(u) &= B_0 + \sum_{i=1}^{n_B} \left\{ B_{2i-1,c} \cos(2i-1)\Delta u \right. \\ &\quad \left. + B_{2i-1,s} \sin(2i-1)\Delta u \right\}. \end{aligned} \tag{5}$$

The extended ECOM has user-defined upper limits n_D, and n_B. Note that the angular argument Δu of the new ECOM is independent of the coordinate system used.

For $n_D = 0$ and $n_B = 1$, model (5) is equivalent to the reduced ECOM (4). Using Δu as angular argument allows for a much better intuitive interpretation of the estimated parameters, because it keeps the reference for the phase of the periodic parameters stable in time, independent of the yearly movement of the Earth (together with the satellite constellations) around the Sun. When neglecting the (rather slow) motion of the Sun during the time period of the arc (in general one to few days), one may approximately calculate the coefficients of the new ECOM (5) from those of the old one (4) by approximating the argument of latitude of the Sun u_s by its value in the center of the arc. The result is

$$\begin{aligned} B_{1,c} &= +\cos u_s B_c + \sin u_s B_s \\ B_{1,s} &= -\sin u_s B_c + \cos u_s B_s, \end{aligned} \tag{6}$$

which allows obtaining the new coefficients from already existing old ones a posteriori. Note that the usage of the new angular argument was already suggested by Springer et al. (1999a) in the context of the generation of an empirical a priori SRP model.

For satellites symmetric w. r. t. the spacecraft-fixed coordinate planes we expect the functions $D(u)$ and $B(u)$ to be symmetric w. r. t. the point $u = u_s$. When using the new angular argument $\Delta u = u - u_s$ in the expansion (5), the coefficients $D_{i,s}$ and $B_{i,s}$ of the antisymmetric sine terms must therefore be zero. This statement only holds for satellites with perfect attitude and when taking only direct SRP into account. In practice, there are no perfectly symmetric satellites and no perfect attitude and there is indirect SRP. Therefore, we currently solve for the sine terms in D and B, but expect that they are small. Experience with the new ECOM in the CODE routine analysis will show to what extent this is true and whether additional terms might be required.

5 The extended ECOM for multi-GNSS analysis

Motivated by the theoretical insights of Sect. 4, a number of new candidate ECOMs was assessed regarding the quality of the resulting orbits, station coordinates, and geodynamically relevant parameters (ERPs and geocenter coordinates).

Table 4 Candidate ECOMs

Sol	D_{2pr}	D_{4pr}	B_{1pr}	# par
D2B0	yes	no	no	5
D2B1g	yes	no	GPS	5(R), 7(G)
D2B1	yes	no	yes	7
D4B1	yes	yes	yes	9
COF (D0B1)	no	no	yes	5

Table 4 characterizes these candidate ECOMs and the solution series generated with them. It also contains, as a reference, CODE's final one-day solution COF, generated in the framework of the IGS Repro-02 initiative (Dach et al. 2014). All solutions are based on the same set of observations gathered by the global station network analyzed routinely by the CODE analysis center of the IGS in 2012 and 2013. The CODE analysis is based on more than 250 stations; it rigorously combines GPS and GLONASS (70–75 % combined receivers in 2012–13), and it uses state-of-the-art background models to account for tropospheric refraction, tidal loading, etc., as described by Dach et al. (2009, 2014). It is important to note that CODE is resolving carrier-phase ambiguities not only for GPS, but also for GLONASS (Dach et al. 2012).

The names of the solution series indicate the highest orders in D and B included in the general representation (5) of the extended ECOM. In this notation, the COF solution could be labeled D0B1. Table 4 lists the solutions in ascending order of the number of ECOM parameters, which have to be estimated per satellite. This order is retained in the tables listing the spectral lines of solutions or of solution differences.

Because the absence of periodic terms in D is a major deficit of the present ECOM, all of the candidate ECOMs contain at least 2pr terms in D. The results of Sect. 3 showed that periodic terms in B may degrade the geocenter coordinates and ERPs, in particular for GLONASS. Although no periodic terms in D were estimated there and despite the theoretical predictions we have added two solutions without periodic terms in B, D2B0 and D2B1g, where the latter contains the terms for the GPS satellites only. The 3-parameter ECOM of Sect. 3.2, which, in the notation introduced, would be labeled D0B0, was assessed as well. However, except for generating rather smooth geocenter z-coordinates, the other resulting geodynamical parameters and the orbits are degraded w. r. t. the other candidate ECOMs. D0B0, therefore, is not considered anymore for the following investigations.

5.1 Geocenter coordinates

Figure 9 shows the estimated geocenter z-coordinates of the candidate series. Figures of the x- and y-coordinates of the geocenter are not provided, because different solutions result

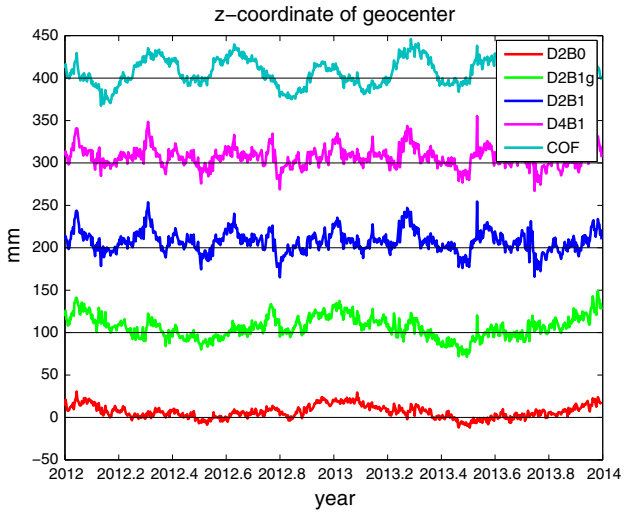

Fig. 9 Geocenter z-coordinate as determined in the candidate ECOM series. All but D2B0 coordinates are vertically shifted by 100 mm w. r. t. each other

Table 5 Amplitudes (in mm) of the geocenter coordinates

Sol	Par	3 cpy	2 cpy	1 cpy
D2B0	x	1	1	2
D2B1g	x	0	1	3
D2B1	x	1	1	3
D4B1	x	1	1	2
COF	x	2	1	3
SLR	x	0	1	3
D2B0	y	0	0	5
D2B1g	y	1	2	4
D2B1	y	1	0	4
D4B1	y	1	3	4
COF	y	1	1	5
SLR	y	0	0	3
D2B0	z	3	1	8
D2B1g	z	5	2	14
D2B1	z	10	2	4
D4B1	z	8	2	4
COF	z	18	1	9
SLR	z	0	1	4

in almost undistinguishable x- and y-coordinates, indicating that the x- and y-coordinates of the geocenter are almost independent of the particular orbit model. Table 5 lists the amplitudes of the spectral lines at 3, 2, and 1 cpy for all candidate series and COF.

In the z-coordinate of the geocenter the COF series shows a pronounced signal at 3 cpy with an amplitude of 18 mm. All candidate solutions considerably reduce the amplitude of this supposedly spurious term. It is in particular remarkable

that the addition of the 2pr term in solution D2B1 reduces the signal by almost a factor of two w. r. t. COF!

In accordance with the findings in Sect. 3.2 the z-coordinate becomes much smoother if no periodic B terms are estimated: the reduction of the 3 cpy term to about 3 mm is most pronounced for the solution D2B0. The solution D2B1g, including the 1pr terms in B only for the GPS, shows the second smallest amplitude at 3 cpy. However, solutions D2B0 and D2B1g show a sizable annual signal.

The COF solution corresponds to the case ('CMB', $B_{1\mathrm{pr}} =$ yes) in Sect. 3.2. The values of the amplitudes slightly differ (Table 1), because the results in Sect. 3.2 were obtained using data from 92 well-selected combined GPS/GLONASS receivers, whereas for the COF solution also data from GPS-only receivers were used and GLONASS thus has a slightly reduced impact.

Due to geophysical processes the geocenter coordinates are not expected to be zero. Sośnica et al. (2014) analyzed geocenter motion using satellite laser ranging (SLR) observations. Table 5 also contains the resulting amplitudes of the SLR-derived geocenter coordinates. The latter are available only from seven-day solutions, which is why the corresponding time series is not shown in Fig. 9. Note that estimating 1pr terms in B for both GPS and GLONASS obviously renders the yearly signal in the GNSS-derived geocenter motion in z more realistic (although increasing the 3 cpy amplitude compared to solutions without the B terms). Solutions D2B1 and D4B1, therefore, show annual signals which best match the SLR-derived values. Note, as well, that the SLR- and GNSS-determinations of the x- and y-coordinates agree very well.

5.2 Earth rotation parameters

Currently, the geocenter coordinates are not IGS products, but the ERPs are. From the IGS perspective the quality of the ERPs is, therefore, more important than that of the geocenter coordinates.

Tables 6 and 7 summarize the amplitude differences of the x- and y-coordinates of the pole and of the LOD w. r. t. the IERS 08 C04 series. As the amplitudes should be zero we also include the sum of these quantities. As in Sect. 3.2, we do not use the estimated polar motion drifts as a quality indicator for the orbit models, because one-day solutions cannot contribute on a scientifically interesting level to these drifts.

Compared to COF, the addition of periodic terms in D reduces the amplitudes at nearly all periods considered. Exceptions are the annual period, which becomes slightly larger for most solutions, and the x-coordinate at 2 and 4 cpy.

In view of the fact that the RMS errors of the C04 pole coordinates and LOD are today of the order of 30 μas and 15 μs/day,[1] respectively, we conclude that all solutions, including COF, qualify as valuable contributors to the IERS 08 C04 series.

Table 6 Amplitudes of polar motion differences (in μas) w. r. t. IERS 08 C04

Sol	Par	4 cpy	3 cpy	2 cpy	1 cpy	Sum
D2B0	x	3	6	9	7	25
D2B1g	x	4	12	3	11	30
D2B1	x	5	8	5	15	33
D4B1	x	5	7	4	15	31
COF	x	0	16	4	13	33
D2B0	y	1	6	5	14	26
D2B1g	y	3	9	2	13	27
D2B1	y	1	6	0	13	20
D4B1	y	1	6	0	14	21
COF	y	3	12	4	10	29

Table 7 Amplitudes (in μs/day) of the ECOM candidates' LOD differences w. r. t. IERS 08 C04

Sol	4 cpy	3 cpy	2 cpy	1 cpy	Sum
D2B0	1.7	1.5	3.3	1.9	8.4
D2B1g	1.8	1.6	4.2	4.1	11.7
D2B1	2.9	1.4	4.1	3.0	11.4
D4B1	2.9	0.9	4.5	2.8	11.1
COF	4.0	3.2	5.1	1.9	14.2

Regarding the sum of the amplitudes, the differences between the estimated ERP series and IERS 08 C04 series are best for x and LOD if no 1pr terms in B are included, the solution D2B1g performs slightly worse. The differences in the y pole coordinate become smaller when including the periodic B terms as well. The differences between the solutions D4B1 and D2B1 are marginal; it seems to be slightly advantageous to add the 4pr term to the estimated orbit parameters.

Small differences between the amplitudes of the COF solution and the ('CMB', $B_{1\mathrm{pr}} =$ yes) solution in Sect. 3.2 can be explained by the station selections of the two solutions.

5.3 Station coordinates

The station coordinates are estimated using a minimum constraint solution (no-net-rotation and no-net-translation conditions) on a verified list of reference sites from the IGb08 reference frame. Each individual daily solution is compared with the linearly extrapolated reference frame coordinates applying a Helmert transformation.

Figure 10 shows the amplitude spectra of the scale parameter for the five different solution types. At the 1 and 3 cpy frequencies we can find the biggest difference between the

[1] ftp://hpiers.obspm.fr/iers/eop/eopc04/C04.guide.pdf.

solutions. At 3 cpy there is a reduction of the amplitude of about 30 % for D2B1 and D4B1 w. r. t. the other solutions. For the annual period a slight increase is visible for all solutions—the smallest (∼6 %) is induced by solution D4B1.

The coordinate repeatability during the 2-year period differs only marginally between the five solution types, because the repeatability is dominated by other variations of the station coordinates in time, e. g., by loading effects.

5.4 Orbits

The vector misclosures of the satellite positions at the day boundaries serve as a measure of orbital accuracy. The mean values of these overlaps over the 2 years of estimated orbits are illustrated in Fig. 11, separately for GPS and GLONASS satellites. The COF solution and solutions D2B0 and D2B1g are worst in the orbit misclosures: D2B1 and D4B1 are approximately on the same level. The differences are, however, small: the extended ECOM improves the orbit misclosures by about 10 %, a clear, but not an overwhelming improvement.

Apart from the orbit misclosures—indicating the internal orbit accuracy—differences to orbits of other analysis centers were analyzed. Table 8 shows the mean RMS errors of the daily Helmert transformations between the orbits of COF, D2B1 and D4B1 on the one hand and the operational orbits of IGS (merged final GPS and GLONASS products), GFZ and ESA on the other hand. The line ES2 contains the comparison to the orbits computed by ESA in the reprocessing campaign, in which the box-wing model of Rodríguez-Solano (2014a) was used as a priori model (Springer et al. 2014). All selected analysis centers provide GLONASS orbits. For the left part of Table 8 only GPS orbits were taken into account, while for the right part GPS and GLONASS orbits were compared. Regarding all orbits, a switch from the COF solution to an extended ECOM reduces the consistency to all external orbits. This is expected, because the extended ECOM is supposed to reduce systematic orbit errors present in the reference orbits. Note that the smallest increase in orbit differences is found for the ES2 solution. For the GPS orbits only, there is even a slight improvement of consistency w. r. t. ES2 with the extended ECOM.

Based on the analysis of geocenter coordinates, ERPs, station coordinates, and orbits, we conclude that the new extended ECOM must have both, the 2pr term in D and the

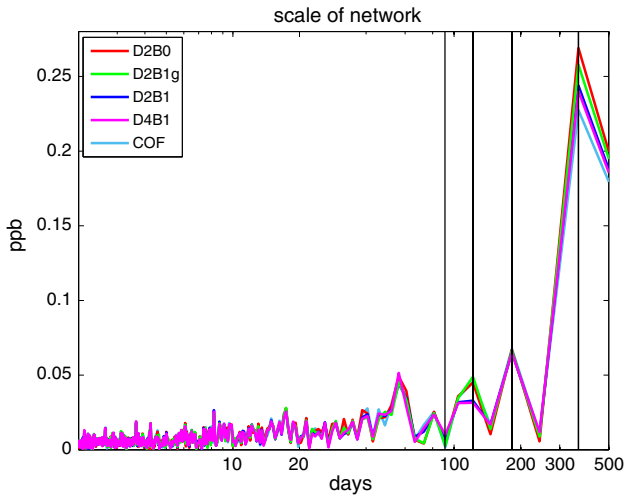

Fig. 10 Amplitude spectra of the scale parameter of a seven-parameter Helmert transformation between the estimated coordinates and the extrapolated IGb08 reference coordinates

Table 8 Mean RMS errors (in mm) of daily Helmert transformations between candidate ECOM solutions and external orbits

	GPS			GPS+GLO		
	COF	D2B1	D4B1	COF	D2B1	D4B1
IGS	13.2	18.8	20.0	24.6	35.6	35.8
GFZ	15.7	21.9	22.8	30.2	41.3	40.7
ESA	11.8	18.9	20.1	29.1	40.7	40.0
ES2	17.0	15.5	16.9	27.0	31.0	31.2

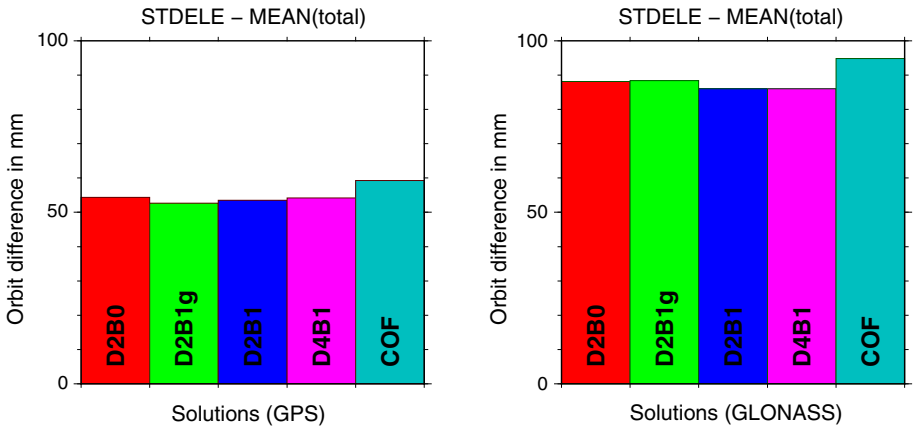

Fig. 11 Mean 3-dimensional misclosures of the daily orbits at the day boundaries for the GPS (*left*) and the GLONASS (*right*) satellites

1pr term in B (for GPS and GLONASS). The above results identify the solutions D2B1 and D4B1 as top candidates for the new ECOM, slightly favoring D4B1 over D2B1. It is remarkable that the sole addition of the absolutely mandatory 2pr term in D to the currently used ECOM (4) already considerably improves the quality of basically all of the assessed estimates.

6 Validation of GNSS orbits with SLR

SLR provides an independent validation and may be used to assess the quality of GNSS orbits. The advantage of SLR lies in the absolute range information, which is virtually free from systematic effects related to ionosphere and troposphere delays, phase ambiguities, and clocks. Therefore, SLR observations are contaminated by only a few error sources.

Unfortunately, only two GPS Block IIA satellites were equipped with Laser Retroreflector Arrays (LRA), namely GPS-36 (decommissioned in April 2014) and GPS-35 (decommissioned in May 2013). As opposed to that, all GLONASS satellites are equipped with LRA.

The SLR range residuals are computed as differences between the SLR observations and the distances derived from the microwave orbits. The station coordinates are fixed to the a priori reference frame SLRF2008. The SLR observations are corrected for relativistic effects, troposphere delays, and for the offset of LRA w. r. t. the satellites' centers of mass.

The SLR residuals serve as an indicator for the radial accuracy of the microwave-derived orbits, because the maximum angles of incidence of a laser pulse to a satellite are only about 13° and 14° for GPS and GLONASS satellites, respectively.

Fritsche et al. (2014) studied the dependence of the mean SLR biases for GLONASS on different elevation angles of the Sun above the orbital plane on the basis of multi-year GNSS solutions. The maximum positive bias of approximately +60 mm was obtained for $\beta_s = \pm 20°$ and $\Delta u = u - u_s \approx 180°$. Furthermore, a maximum negative bias was found for $\Delta u \approx 0°$. A similar behavior is observed in all solutions, which do not solve for 2pr parameters in D direction, see, e. g., the COF solution in Fig. 12.

Figure 13 illustrates that the estimation of the 2pr terms in D greatly reduces the spurious pattern of the SLR residuals as a function of β_s and Δu. As a result, the estimated microwave orbits become almost unaffected by artifacts related to SRP modeling deficiencies. The RMS error of the SLR observations (RMS around the mean value) is reduced from 34.6 to 32.1 mm, i. e., by 7 % and the mean bias of GLONASS becomes comparable to that of the GPS satellites. The remaining biases between SLR and GNSS solutions originate mainly from the satellite signature effect, which is caused by a spread of the laser pulse due to reflection from multiple reflectors in the LRA. The satellite signature effect can be as large as 15 mm for multi-photon SLR detectors when ranging to GLONASS-M satellites (Sośnica et al. 2015).

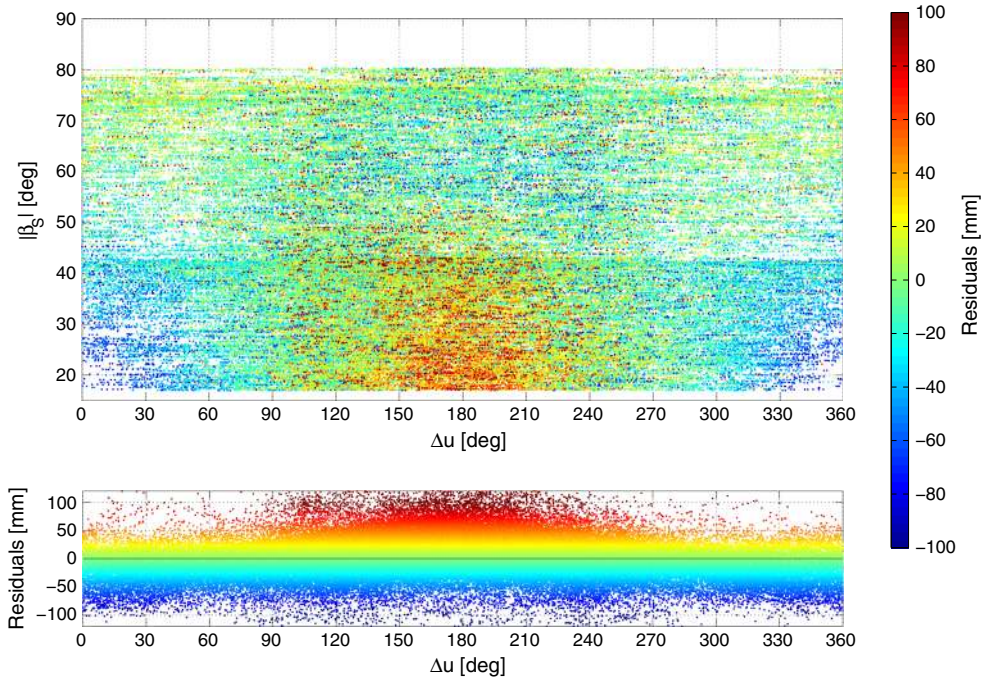

Fig. 12 Residuals of SLR observations to GLONASS satellites in 2012–2013 for COF solution (in mm). The observations for eclipsing satellites and for the satellites R11 (SVN 723) and R21 (SVN 725) were excluded

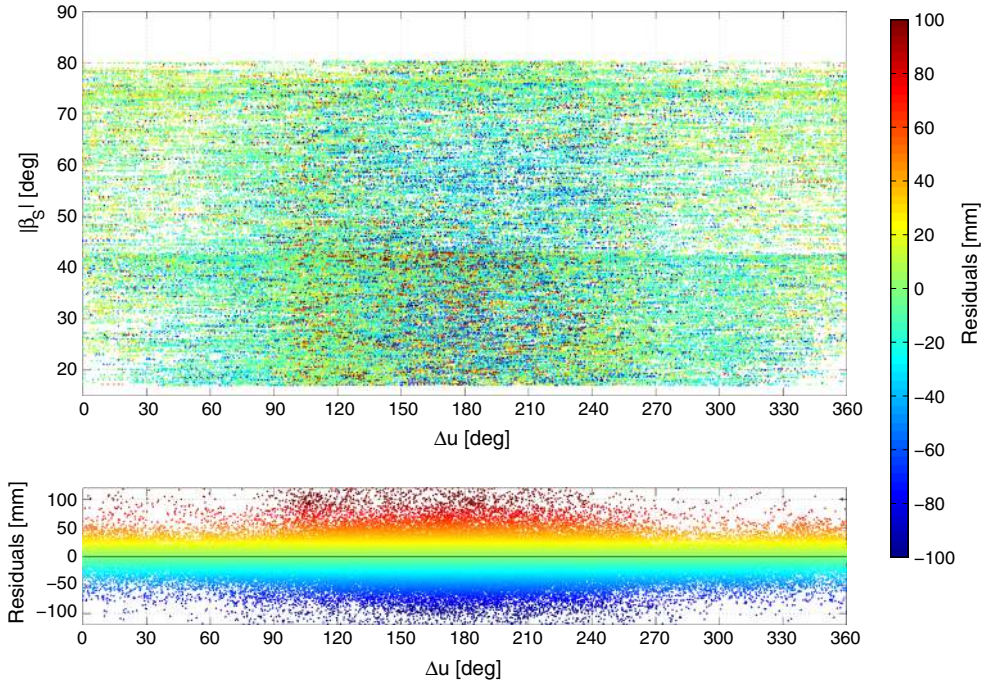

Fig. 13 Residuals of SLR observations to GLONASS satellites in 2012–2013 for D2B1 solution (in mm). The observations for eclipsing satellites and for the satellites R11 (SVN 723) and R21 (SVN 725) were excluded

Table 9 GNSS orbit validation using SLR observations (values in mm)

Solution	GPS Block IIA		GLONASS-M	
	Mean bias	RMS	Mean bias	RMS
D2B0	−6	25	−6	32
D2B1g	−10	24	−6	32
D2B1	−10	24	−6	32
D4B1	−10	24	−7	33
COF	−12	25	1	35

For the two GPS satellites the RMS error of SLR observations is reduced from 25.3 for COF to 23.6 mm for D2B1, i. e., by 9 %. The dependency of the SLR residuals on Δu is different than that observed for GLONASS, i. e., the maximum negative residuals occur at $\Delta u \approx 180°$ and not at $\Delta u \approx 0°$. The SLR validation shows, however, that this pattern is reduced, as well, for GPS satellites.

Table 9 summarizes the mean offsets and RMS values of the SLR residuals w. r. t. microwave GNSS orbits for all assessed solutions. For GPS the smallest RMS values of SLR residuals are obtained for the solutions D2B1, D4B1, and D2B1g. Neglecting the 1pr parameters in B introduces some artifacts into the GPS orbits and increases the RMS value to 25.2 mm in D2B0 (degradation of about 7 % w. r. t. D2B1). For GLONASS the smallest variations of the residuals is obtained for solutions D2B1, D2B0, and D2B1g, whereas D4B1 is degraded by 1 mm in both the mean bias and the RMS. The two GLONASS satellites R11 (SVN 723) and R21 (SVN 725) have been excluded in Figs. 12 and 13 and in the statistics, because their SLR residuals look peculiar and become larger and more systematic when using the extended ECOM. We attribute that to satellite-specific attitude problems.

7 Summary and conclusions

In Sect. 3.2 we analyzed the geocenter coordinates and the ERPs emerging from a GLONASS-only, a GPS-only, and a combined GPS/GLONASS analysis based on a data set gathered by a global network of 92 combined GPS/GLONASS receivers in the years 2009–2011. We first used the so-called reduced ECOM described in Sect. 3.1 for this purpose.

The three solution series generated high-quality geocenter coordinates x and y, which are in the order of magnitude comparable to SLR determinations of the geocenter (Sośnica et al. 2014). It is in particular important that the amplitude at 3 cpy is small, of the order of 1–2 mm. The amplitude at 1 cpy is about a factor of 2 larger than expected by SLR.

The GPS-only solution generates acceptable results in the geocenter coordinate z, as well. The amplitude at 1 cpy is roughly as expected by SLR, the amplitude of 4 mm at 2 cpy is too large (1.3 mm are expected from SLR), and the amplitude of 5 mm at 3 cpy is definitely too large.

The GLONASS-only solution generates heavily biased z-coordinates, which was made known by Meindl et al. (2013). The amplitude of 112 mm at 3 cpy clearly indicates that a GLONASS-specific problem exists. Unfortunately, this bias is also clearly visible in the combined solution with an amplitude of 20 mm at 3 cpy.

When omitting the 1pr term in B, the GLONASS-only and the combined solutions get much better in the z-coordinate, but now the amplitudes at 1 cpy are suffering. In summary, from the point of view of the geocenter, the 3-parameter ECOM without periodic terms is much better for the GLONASS and the combined solutions, but not sufficient when striving for highest accuracy.

The validation of the ERPs derived from the three solution series in Sect. 3.2 in essence confirms the result obtained for the z-coordinate of the geocenter: the GPS-only solution achieved with the 5-parameter ECOM does not show obvious biases. Even the sum of the four spectral lines at 1, 2, 3, and 4 cpy for the x- and y-coordinates of the pole lies roughly within the RMS error of the IERS 08 C04 series. The GLONASS-only solution based on the 5-parameter ECOM is heavily deteriorated. The problem is—as in the case of the z-coordinate of the geocenter—the signal at 3 cpy: amplitudes of 210 and 70 μas at 3 cpy are simply unrealistic. The LOD estimates confirm the results of the pole coordinates, where the problematic amplitudes are at the 4 and 2 cpy frequencies.

As in the case of the geocenter z-coordinate, the 3-parameter ECOM improves the quality of the pole coordinates and of LOD.

Direct SRP acceleration acting on a GNSS satellite body was analyzed in Sect. 4. For simple satellite bodies in yaw-steering mode it was argued that only even-order terms should exist in the D-component of the ECOM and only odd-order terms in B.

This hypothesis was tested using the box-wing models by Rodríguez-Solano (2014a) and the older ROCK-T models documented in Fliegel et al. (1992, 1996). Both model types largely meet the expectations. As a result of these investigations the extended ECOM was given the form (5).

The reduced 5-parameter ECOM (4) is a member of the new extended ECOM family defined by Eq. (5), whereas the full ECOM, represented by Eq. (3) is not.

The new ECOM uses the angle $\Delta u \doteq u - u_s$ as argument and no longer simply u. The differences are negligible for one-day arcs, see Eq. (6), for longer arcs of, let us say, one week the difference might matter, in particular for small values of $|\beta_s|$. In any case the new angular argument is much better suited for interpreting the estimated ECOM parameters.

Four ECOM candidates (Table 4) were validated in Sect. 5 using the same criteria as in Sect. 3.2 and in addition also the quality of orbits and station coordinates. All candidates contained 2pr terms in D, one even the 4pr terms. Three candidates contained the 1pr terms in B, one only for GPS.

All candidate solutions are performing on the level expected by SLR when considering the x- and y-coordinates of the geocenter. The bias at 3 cpy in the z-coordinate did not completely disappear, but it was reduced by factors varying between 2 to 6. Unfortunately, the best solutions at 3 cpy have relatively high (thus less realistic) amplitudes at 1 cpy.

All solutions generate pole coordinates and LOD values superior to the COF solution, using the IERS 08 C04 as reference. For the pole coordinates, the new solutions (with the exception of D2B0) slightly increase the amplitude of the annual period as compared to COF.

The orbits were assessed by comparing the orbit misclosures at the day boundaries. In these tests COF, D2B0, and D2B1g gave the worst results; the other solutions slightly reduce the discrepancies. Furthermore, the orbits were compared to orbits provided by other analysis centers. Overall, the consistency to the external orbits is degraded when switching from the old to the updated ECOM. The smallest degradation is observed w.r.t. the orbits of the reprocessing campaign of ESA, where the box-wing model of Rodríguez-Solano (2014a) was used. Considering GPS orbits only, there is even a slight improvement of consistency to these ESA orbits when using the extended ECOM.

The station coordinates were analyzed by computing spectra of the scale parameter of a Helmert transformation between the daily coordinate estimates and the extrapolated IGb08 reference coordinates. The effect of different orbit models on the coordinates turned out to be rather small.

Finally, the candidate solutions were validated using the SLR technique in Sect. 6. The results are convincing and show that the spurious patterns in SLR residuals are reduced by the new candidate ECOMs.

The microwave carrier phase residuals are comparatively insensitive to the orbit parametrization: the mean value of the ionosphere-free phase residual RMS over the two processed years 2012 and 2013 is 4.130 mm for COF and 4.101 mm for D4B1.

In summary, the assessments identify the solutions D2B1 and D4B1 as top candidates for the new extended ECOM, slightly favoring D4B1 over D2B1. Based on our experiments we recommend current users of the classic 5-parameter ECOM analyzing GLONASS to switch to either the modified model D2B1 or to D4B1.

As a result of the review of the ECOM performed in this article the CODE IGS contributions are based on solution D4B1 since January 4, 2015.

A reprocessing of data of 2014 and an analysis of the now routinely generated solutions based on D4B1 will enable an improved evaluation of the new ECOM. This allows maintaining the performance of the proposed extended ECOM—

updates may be needed in the future—and will be in particular useful when addressing eclipsing satellites, which were not in the focus of our interest here.

References

Bar-Sever Y (1996) A new model for GPS yaw attitude. J Geod 70:714–723. doi:10.1007/BF00867149

Bar-Sever Y, Kuang D (2004) New empirically derived solar radiation pressure model for global positioning system satellites. IPN Progress Report 42–159, Nov 15, 2004

Beutler G, Brockmann E, Gurtner W, Hugentobler U, Mervart L, Rothacher M, Verdun A (1994) Extended orbit modeling techniques at the CODE processing center of the International GPS Service for geodynamics (IGS): theory and initial results. Manuscr Geod 19:367–384

Bizouard C, Gambis D (2009) The combined solution C04 for Earth orientation parameters consistent with international terrestrial reference frame 2005. Int Assoc Geod Symp 134. doi:10.1007/978-3-642-00860-3_41

Dach R, Hugentobler U, Meindl M, and Fridez P (eds) (2007) The Bernese GPS Software Version 5.0, Astronomical Institute, University of Bern

Dach R, Brockmann E, Schaer S, Beutler G, Meindl M, Prange L, Bock H, Jäggi A, Ostini L (2009) GNSS processing at CODE: status report. J Geod 83(3–4):353–366

Dach R, Schaer S, Lutz S, Bock H, Orliac E, Prange L, Thaller D, Mervart L, Jäggi A, Beutler G, Brockmann E, Ineichen D, Wiget A, Weber G, Habrich H, Ihde J, Steigenberger P, Hugentobler U (2012) Annual Center Reports: Center for Orbit Determination in Europe (CODE). pp. 29–40. In: Meindl M, Dach R, Jean Y, Astronomical Institute, University of Bern (eds) International GNSS Service, Technical Report 2011, printed by IGS Central Bureau, Pasadena, California (USA)

Dach R, Schaer S, Lutz S, Baumann C, Bock H, Orliac E, Prange L, Thaller D, Mervart L, Jäggi A, Beutler G, Brockmann E, Ineichen D, Wiget A, Weber G, Habrich H, Söhne W, Ihde J, Steigenberger P, Hugentobler U (2014) Annual Center Reports: Center for Orbit Determination in Europe (CODE). pp. 21–34. In: Dach R, Jean Y, Astronomical Institute, University of Bern (eds) International GNSS Service, Technical Report 2013, printed by IGS Central Bureau, Pasadena, California (USA)

Dow J, Neilan R, Rizos C (2009) The International GNSS Service in a changing landscape of global navigation satellite systems. J Geod 83(3–4):191–198. doi:10.1007/s00190-008-0300-3

Fliegel HF, Gallini TE, Swift ER (1992) Global positioning system radiation force model for geodetic applications. JGR 97(B1):559–568

Fliegel HF, Gallini TE (1996) Solar force modeling of block IIR global positioning system satellites. J Spacecr Rockets 33(6):863

Fritsche M, Sośnica K, Rodríguez-Solano CJ, Steigenberger P, Dietrich R, Dach R, Wang K, Hugentobler U, Rothacher M (2014) Homogeneous reprocessing of GPS, GLONASS and SLR observations. J Geod 88(7):625–642. doi:10.1007/s00190-014-0710-3

Griffith J, Ray JR (2012) Sub-daily alias and draconitic errors in the IGS orbits. GPS Solut. doi:10.1007/s10291-012-0289-1

Hefty J, Rothacher M, Springer TA, Weber R, Beutler G (2000) Analysis of the first year of Earth rotation parameters with a sub-daily time resolution gained at the CODE processing center of the IGS. J Geod 74:479–487

Meindl M (2011) Combined analysis of observations from different global navigation satellite systems. Geodätisch-geophysikalische Arbeiten in der Schweiz, vol 83, Eidg. Technische Hochschule Zürich, Switzerland

Meindl M, Beutler G, Thaller D, Jäggi A, Dach R (2013) Geocenter coordinates estimated from GNSS data as viewed by perturbation theory. Adv Space Res 51(7):1047–1064. doi:10.1016/j.asr.2012.10.026

Montenbruck O, Steigenberger P, Hugentobler U (2014) Enhanced solar radiation pressure modeling for Galileo satellites. J Geod. doi:10.1007/s00190-014-0774-0

Pearlman MR, Degnan JJ, Bosworth JM (2002) The international laser ranging service. Adv Space Res 30(2):135–143. doi:10.1016/S0273-1177(02)00277-6

Ray J, Altamimi Z, Collilieux X, van Dam T (2008) Anomalous harmonics in the spectra of GPS position estimates. GPS Solut 12:55–64. doi:10.1007/s10291-007-0067-7

Ray J, Griffiths J, Collilieux X, Rebischung P (2013) Subseasonal GNSS positioning errors. Geophys Res Lett (GRL). doi:10.1002/2013GL058160

Rodríguez-Solano CJ, Hugentobler U, Steigenberger P, Lutz S (2011) Impact of Earth radiation pressure on GPS position estimates. J Geod. doi:10.1007/s00190-011-0517-4

Rodríguez-Solano CJ (2014) Impact of non-conservative force modeling on GNSS satellite orbits and global solutions. Ph. D. thesis, Technical University of Munich

Rodríguez-Solano CJ, Hugentobler U, Steigenberger P, Blossfeld M, Fritsche M (2014b) Reducing the draconitic errors in GNSS geodetic products. J Geod 88:559–574. doi:10.1007/s00190-014-0704-1

Sośnica K, Jäggi A, Thaller D, Dach R, Beutler G (2014) Contribution of Starlette, Stella, and AJISAI to the SLR-derived global reference frame. J Geod 88(8):789–804. doi:10.1007/s00190-014-0722-z

Sośnica K, Thaller D, Dach R, Steigenberger P, Beutler G, Arnold D, Jäggi A (2015) Satellite laser ranging to GPS and GLONASS. J Geod. doi:10.1007/s00190-015-0810-8

Springer TA, Beutler G, Rothacher M (1999a) A new solar radiation pressure model for GPS satellites. GPS Solut 3(2):50–62

Springer TA (1999b) Modeling and validating orbits and clocks using the global positioning system. Geodätisch-geophysikalische Arbeiten in der Schweiz, vol 60, Eidg. Technische Hochschule Zürich, Switzerland. ISBN-978-3-908440-02-4

Springer TA, Flohrer C, Otten M, Enderle W (2014) ESA reprocessing: advances in GNSS analysis. IGS workshop 2014, California, USA

Ziebart M, Cross P, Adhya S (2002) Modeling photon pressure: the key to high-precision GPS satellite orbits. GPS World 13(1):43–50

Ziebart M (2004) Generalized analytical solar radiation pressure modeling algorithm for spacecraft of complex shape. J Spacecr Rockets 41(5):840–848. doi:10.2514/1.13097